Received: 13 August 2019 | Revised: 12 October 2019 | Accepted: 6 November 2019

DOI: 10.1096/fj.201902039R

RESEARCH ARTICLE

THE FASEB JOURNAL

DDIT4 gene expression is switched on by a new HDAC4 function in ataxia telangiectasia

Anastasia Ricci | **Luca Galluzzi** | **Mauro Magnani** | **Michele Menotta**

Department of Biomolecular Sciences, University of Urbino "Carlo Bo", Urbino, Italy

Correspondence
Anastasia Ricci, Department of Biomolecular Sciences, University of Urbino "Carlo Bo", Via Saffi 2, 61029 Urbino, Italy.
Email: anastasia.ricci@uniurb.it

Funding information
EC | Horizon 2020 (EU Framework Programme for Research and Innovation), Grant/Award Number: 667946; FanoAteneo

Abstract

Ataxia telangiectasia (AT) is a rare, severe, and ineluctably progressive multisystemic neurodegenerative disease. Histone deacetylase 4 (HDAC4) nuclear accumulation has been related to neurodegeneration in AT. Since treatment with glucocorticoid analogues has been shown to improve the neurological symptoms that characterize this syndrome, the effects of dexamethasone on HDAC4 were investigated. In this paper, we describe a novel nonepigenetic function of HDAC4 induced by dexamethasone, through which it can directly modulate HIF-1a activity and promote the upregulation of the DDIT4 gene and protein expression. This new HDAC4 transcription regulation mechanism leads to a positive effect on autophagic flux, an AT-compromised biological pathway. This signaling was specifically induced by dexamethasone only in AT cell lines and can contribute in explaining the positive effects of dexamethasone observed in AT-treated patients.

KEYWORDS

ataxia telangiectasia, DDIT4, dexamethasone, HDAC4

1 | INTRODUCTION

Ataxia telangiectasia (AT) is a rare neurodegenerative disease caused by biallelic mutations in the ataxia telangiectasia-mutated (ATM) gene (Chr 11q22.3-23.1), which encodes for the ATM protein, a member of the PI3 kinase-like kinase (PIKK) family.[1,2]

AT patients show a complex phenotype characterized primarily by an early onset progressive cerebellar ataxia, loss of Purkinje cells, oculocutaneous telangiectasias, immunodeficiency, proneness to the development of tumors (lymphoma and leukemia) and infections (respiratory infections).[3-6]

Ataxia telangiectasia-mutated, initially discovered as a protein with nuclear functions, as it is activated after DNA damage,[7,8] modulating cell cycle-checkpoint signaling,[9] also has pleiotropic effects in the cytoplasm. These effects are still under investigation.[10-15]

Unfortunately, there is currently no cure available for AT patients, but only supportive therapies to ameliorate their pain. However, in the last few years, observational studies and clinical trials have shown that treatment with glucocorticoid analogues improves the neurological symptoms of AT patients, although their mechanism of action have only partially been elucidated.[16-20] The limitations observed with the use of oral corticosteroids, leading to undesirable side effects have been overcome with the administration of a sustained released delivery system via patients' red blood cells.[16,17] Several studies have been carried out in order to gain insight into the

Abbreviations: AT, ataxia telangiectasia; dex, dexamethasone; DMSO, dimethylsulfoxide; hTERT, human telomerase reverse transcriptase; qPCR, quantitative PCR; TFs array, transcription factors array; MEM, minimum essential medium; PPIC and PPIA, peptidylprolyl isomerase A and C.

biological effects of glucocorticoids in AT patients and in cellular models, highlighting their role in redox balance, gene expression, protein regulation, and organelle dynamics.[21-27] Li et al reported the role of ATM in balancing HDAC4 function in AT neurons.[28] Among class II HDACs, HDAC4 is implicated in the control of gene expression, and it is also important for several cellular functions and is the major player in synaptic plasticity.[29] HDAC4 is expressed particularly in the heart, skeletal muscle, and in the brain, where it seems to be predominantly localized in the cytoplasm.[30,31] Loss of HDAC4 cytoplasmic distribution induces neuronal cell death. HDAC4 is normally phosphorylated by calcium/calmodulin-dependent kinases (CaMKs), enabling its binding to the chaperones 14.3.3 protein family, and leading to its nuclear export while preventing its nuclear import.[32-34] Protein phosphatase 2A (PP2A) in turn, regulates the de-phosphorylation of HDAC4, promoting its nuclear shift.[35] A lack of ATM causes the deregulation of PP2A and subsequent HDAC4 nuclear accumulation, inhibiting the transcription factors myocyte enhancer factor 2A (MEF2A) and cAMP response element-binding protein (CREB), thus promoting the repression of neuronal survival genes and leading to neurodegeneration.[28]

In light of the above-mentioned dynamics involved in AT pathology and based on our previous investigations regarding dexamethasone (dex) action in AT cells and patients,[36] we decided to investigate whether dex can alter HDAC4 cellular localization and function in AT fibroblast cell lines. Dexamethasone treatment was found to promote a new non-epigenetic role of HDAC4, consisting in HDAC4 mediated HIF-1a regulation which leads to an ATM-independent DDIT4 transcription involved in the autophagy process that was restored after dex administration. These data can contribute in understanding the beneficial effect of dexamethasone in the treatment of AT.

2 | MATERIALS AND METHODS

2.1 | Cell cultures

Fibroblasts WT AG09429 (ATM+/+) and AT GM00648 (ATM−/−) from Coriell Institute (Camden, NJ, USA) were used as a cellular model. The hTERT antigen cell immortalization Kit (Alstem Cell Advancements) was used to immortalize the cells. The selected AT GM00648 hTERT (AT 648 hT) and WT AG09429 hTERT (WT hT) were grown in MEM (Eagle formulation). The medium was supplemented with 2 mmoL/L L-glutamine, 100 U/mL penicillin, and 0.1 mg/mL streptomycin (Sigma Aldrich), 10% fetal bovine serum (Thermo Fisher Scientific), and 10 mM glucose. All cells were incubated at 37°C with 5% CO_2 and treated with 100 nM dex for 48 hours prior to each analysis. Dimethylsulfoxide (DMSO) was used as the drug vehicle and thus was administered in untreated cells as a control.

2.2 | Western blotting

Total proteins were extracted using the Protein Extraction Reagent Type 4 (P4, Sigma Aldrich). Cells were sonicated with 10 pulses of 15 seconds at 45 Watts Labsonic 1510 Sonicator (Braun) and clarified by centrifugation for 10 minutes at 10 000 RCF. Cytosolic and nuclear fractions were obtained lysing the cells in Buffer A (10 mM Hepes/KOH pH 7.9, 1.5 mM $MgCl_2$, 10 mM KCl, 1 mM dithiothreitol (DTT), 0.1% Nonidet-P40) completed with protease inhibitors (Roche Applied Science) and phosphatase inhibitors (10 mM NaF, 2 mM Na_3VO_4) in ice for 10 minutes. Cells were centrifuged at 5000 RCF for 10 minutes and the supernatants containing the cytosolic fraction were collected. The pellets were then lysed in P4 and sonicated for 10 pulses of 10 seconds at 45 Watts. After clarification, the supernatants containing the nuclear fractions were collected. Protein concentration was determined by the Bio-Rad Protein Assay, based on Bradford's method.

Twenty micrograms of proteins were separated by SDS-PAGE according to the Laemmli protocol[37] (Novex Tris-Glycine gels) and then transferred to nitrocellulose (0.22 µm, Bio-Rad) by wet transfer and Towbin blotting buffer (50 mM Tris, 150 mM NaCl, 20% (v/v) methanol). Membranes were probed with the primary antibodies and corresponding secondary HRP-coupled antibodies diluted in 5% w/v non-fat dry milk or 5% BSA in TBS-T. The following antibodies were used in the analyses : anti-HDAC4 (Cell Signaling Technology CST, Thermo Fisher Scientific, TFS), anti-phospho HDAC4 Ser632 (CST), anti-NFE2L2 (Santa Cruz Biotechnology, SCBT), anti-HIF1-a (CST, TFS), anti-DDIT4 (Bethyl and CST), anti-4E-BP1 (CST) anti-phospho 4E-BP1 Thr37/46 (CST), anti-p70S6K (CST and Bethyl), anti-phospho p70S6K Thr389 (CST), anti-LC3B (CST), anti-SQSTM1/p62 (CST), anti-VPS18 (TFS), anti-AKT (CST) anti-phospho AKT Ser473 (CST), anti-GSK-3a/b (CST), and anti-phospho GSK-3a/b Ser21/9 (CST). Immunoreactive bands were recorded using the enhanced chemiluminescence (Advansta) by ChemiDoc Touch Imaging System (Bio-Rad).

The whole lane normalization strategy was adopted in all western blot analyses using a trihalo compound for protein visualization.[38-40]

Acquired images were analyzed by Image Lab software 5.2.1 (Bio-Rad).[41]

2.3 | Indirect immunofluorescence microscopy

Cells were grown on Lab-Tek II chamber slide (Nunc). After stimulation, they were fixed with 4% formaldehyde for 10 minutes and then with 100% cold methanol for 10 minutes. They were subsequently permeabilized with 0.5% NP-40 in PBS for another 10 minutes.

After performing the blocking procedure for 1 hour at room temperature, primary antibodies were applied in 0.1% Triton X100, 1% BSA in PBS overnight at 4°C. The following antibodies were used: anti-HDAC4 (Cell Signaling Technology, Thermo Fisher Scientific), anti-phospho HDAC4 Ser632 (Cell Signaling Technology), and anti-HIF1-a (Cell Signaling Technology, Thermo Fisher Scientific).

The following day, slides were incubated with secondary anti-mouse TRITC-conjugated antibody (Sigma-Aldrich) or anti-rabbit FITC-conjugated antibody (Sigma-Aldrich) in 0.1% Triton X100, 1% BSA in PBS for 1 hour at 37°C. After washing procedures, DNA was stained with 4′,6-diamidino-2-phenylindole (DAPI) at a final concentration of 0.2 μg/mL. Washed slides were mounted and embedded with ProLong Antifade (Thermo Fisher Scientific). Slides were observed by Olympus IX51, and the images were acquired by ToupCam camera (ToupTek Europe). Image analyses were performed by ImageJ (NIH).

2.4 | Quantitative real-time PCR

Total RNA was extracted from WT hT and AT 648 hT fibroblast cell lines treated with dex or not treated using the RNeasy mini kit (QIAGEN). Five hundred nanograms of RNA were employed in each experiment to obtain cDNA PrimeScript™ RT Master Mix (Takara). One nanogram of cDNA was used in each PCR reaction for TaqMan Gene Expression Assays (Thermo Fisher Scientific) according to the manufacturer's instructions. PPIC and PPIA gene expressions were used as housekeeping genes. Amplification plots were analyzed using the ABI PRISM 7500 sequence detection system (Applied Biosystems) and the relative expression data were calculated by the $½^{\Delta Ct}$ method.

2.5 | HDAC4 cysteines reduction assay

The extent of cysteine reduction in HDAC4 was determined by biotinylated iodoacetamide (BIAM) as reported in Ref. 42,43. Briefly, cells were lysed with Buffer A (10 mM Hepes/KOH pH 7.9, 1.5 mM $MgCl_2$, 10 mM KCl, 0.1% Nonidet-P40), completed with protease inhibitors (Roche Applied Science) and phosphatase inhibitors (10 mM NaF, 2 mM Na_3VO_4) and BIAM 400 μM, in ice for 10 minutes. Nuclei were centrifuged for 10 minutes to collect the supernatant containing the cytosolic fraction. The pellets were resuspended in Ripa Buffer (150 mM NaCl, 50 mM Tris-HCl pH 7.5, 1% NP-40, 0.5% sodium deoxycholate, 0.1% SDS) containing protease and phosphatase inhibitors and BIAM 400 μM. Cells were sonicated with 10 pulses of 15 seconds at 45 Watts in ice and centrifuged for 10 minutes to collect the supernatant containing the nuclear fraction.

The enrichment of reduced proteins was performed with hybridization between 100 μg samples and 60 μL of 50% streptavidin agarose beads (Pierce) in PBS-containing protease inhibitors. The hybridization on a rotating bascule at 4°C lasted for 2 hours. Biotinylated proteins were purified as reported by Rybak et al[44] and subsequently separated by SDS-PAGE (Novex 8%-16%) and transferred to nitrocellulose. Membranes were probed with the primary antibody anti-HDAC4 and immunoreactive signals were detected as previously described.

2.6 | Transcription factors array

Protein nuclear extracts were obtained from WT hT and AT 648 hT cells, with or without dex treatment, extracted in native conditions, according to the recommendations of the Panomics Protein/DNA arrays II kit. Transcription factor activity was evaluated using the enhanced chemiluminescence detection following the manufacturer's instructions.

2.7 | HDAC4 Co-immunoprecipitation

Co-immunoprecipitation of nuclear protein fractions was performed using standard methods. Briefly, cells were lysed in cytosolic lysis buffer (10 mM Hepes, pH7.5, 1.5 mM $MgCl_2$, 10 mM KCl, 10% glicerolo, 0.2% NP-40, 1 mM DDT, and protease inhibitors) in ice for 10 minutes. After centrifugation, nuclei pellet were lysed in nuclear lysis buffer (10 mM Hepes, pH 7.5, 1.5 mM $MgCl_2$, 300mM KCl, 10% glicerolo, 0.2% NP-40, 1 mM DTT protease inhibitors) for 30 minutes at 4°C. Five hundred micrograms of nuclear protein were immunoprecipitated with 3 μg of anti-HDAC4 antibody (CST or TFS) in nuclear lysis buffer at a final concentration of 150 mM KCl. Immunoprecipitates were incubated with Protein A/G agarose beads, at 4°C for 4 hours. Agarose beads were copiously washed in wash buffer (10 mM Hepes, pH7.5, 1.5 mM $MgCl_2$, 150 mM, KCl, 0.25% NP-40, and 10% glycerol). Immunoprecipitated protein complexes were directly boiled in Laemmli's buffer and subjected to western blot analysis as previously described using anti-HDAC3 (CST), anti-14.3.3 ζ/δ (CST), and anti-HIF-1a (CST and TFS).

2.8 | Chromatin immunoprecipitation ChIP

AT 648 hT cells were fixed with 1% formaldehyde at 37°C for 15 minutes, and subsequently the reaction was stopped adding 0.125 mM glycine at room temperature for 5 minutes. Cells were then rinsed with cold PBS, scraped, and centrifuged. To separate the DNA associated with chromatin, pellet was resuspended in 1mL of cell lysis buffer (5 mM HEPES-KOH pH 7.5, 85 mM KCl, 0.5% NP-40,

protease, and phosphatase inhibitors) on ice for 10 minutes and then centrifuged. The obtained pellet was resuspended in nuclear lysis buffer (50mM Tris pH 8, 10mM EDTA, 1% SDS, protease, and phosphatase inhibitors) on ice for 30 minutes. Samples were sonicated with 10-20 pulses of 15 seconds at 45 Watts to achieve a chromatin average size between 200 and 400 base pairs. For ChIP, 10 μg of DNA, 50 μL of 50% agarose-beads, 5 μg of HIF1-a, or HDAC4 antibodies were mixed in 1-mL binding buffer (0.1% SDS, 1% Triton X100, 150 mM NaCl, 2 mM EDTA, 0.5 mM EGTA, 20 mM Tris pH 8, and protease inhibitors) at 4°C overnight. Irrelevant IgG was used as a control. Samples were subsequently centrifuged and washed several times in wash buffer (0.1%SDS, 1% Triton X100, 2 mM EDTA, 150 mM NaCl, 20 mM tris-HCl pH 8) and, lastly, in a final wash buffer (0.1% SDS, 1% Triton X100, 2 mM EDTA, 500 mM NaCl, 20 mM tris-HCl pH8). After centrifugation, the surfactant of each sample was reversed cross-linked in the presence of RNase A, and proteinase K at 65°C overnight and subsequently purified (GenElute PCR clean-up Kit Sigma). Quantitative PCRs were performed using SYBR Green Premix Ex Taq Tli RNaseH Plus (Takara) using the primers surrounding the HIF-1a-binding site in DDIT4 promoter; forward 5′-GTTCGACTGCGAGCTTTCTG–3′, reverse 5′-GCACGTAAGCAACGTTCTCT-3′.

2.9 | Electrophoretic mobility shift assay EMSA

Native nuclear proteins of WT hT and AT 648 hT were extracted as described in the TFs array section and used in EMSA. The double-stranded DNA encompassing the HIF-1a-binding site (TACGTG) of the DDIT4 promoter was obtained and labeled by PCR amplification using 5′FAM modified forward primer 5′-GTTCGAC TGCGAGCTTTCTG-3′ and reverse 5′–CCTTCTCTG CGCCACGACCC-3′.

DNA-protein binding and gel migration were performed as previously reported.[45] Anti-HDAC4 and anti-HIF-1a were added in super shift assays before probe binding.

2.10 | RNA interference

RNAi experiments were performed with 6 nM siRNA against HIF-1a or HDAC4 (Ambion^{R} Silencer^{R} Select Pre-designed siRNAs) using Lipofectamine RNAiMAX (Invitrogen) according the guidelines provided by the manufacturers. The Select Pre-designed scramble 6 nM siRNA was used as a control. SiRNAs were added in the last 24 hours of 48-hour dex stimulation. RNA and proteins were extracted as previously described.

2.11 | Autophagy flux monitoring treatments

In order to analyze the autophagic flux, treated and untreated cells were incubated for 48 hours and subsequently treated with the vehicle (control group), with chloroquine 100 μM (Sigma-Aldrich) and with chloroquine plus Pepstatin A 10 μg/μL (Sigma-Aldrich) for an additional 4 hours. Proteins were then analyzed as previously illustrated.

2.12 | Statistical analysis

GraphPad Prism was used for statistical analyses and graph generation. Statistical tests were chosen according to sample size and variance homogeneity. The following tests were used: *t* test for data from IF experiments, Mann-Whitney U test in case of unpaired medians comparisons, Wilcoxon test in case of paired medians comparisons, and Kruskal-Wallis test (nonparametric ANOVA) when more than two groups were compared. Means or medians were considered statistically different with $P \leq .05$.

3 | RESULTS

3.1 | HDAC4 nuclear accumulation by cysteine reduction

The first aim of this study was to evaluate if dex was able to alter HDAC4 nuclear localization, thus reversing the phenotype induced by its nuclear dysfunction.

The intracellular distribution of HDAC4 (Figure 1A) and p-HDAC4 (Figure 1B) was assayed by indirect immunofluorescence (IF) in both WT hT and AT 648 hT cells treated with dex or untreated. Their quantified amounts are reported in Figures 1C,D, respectively. Consistent with the findings of Li et al, AT cells showed a larger amount of nuclear HDAC4 than did WT cells, and its magnitude further increased only in AT 648 hT after dex stimulation. The amount of nuclear p-HDAC4 was found to be slightly increased (not statistically significant) only in AT cells.

These findings were also verified by western blot analyses of nuclear and total protein extracts using anti-HDAC4 and anti-p-HDAC4 antibodies (Figure 1E). AT 648 hT cells showed an increase in nuclear HDAC4 after stimulation with dex compared to untreated cells. No significant difference was found in WT hT cells in terms of protein quantity (Figure 1F). In agreement with IF quantification, AT 648 hT cells were found to have more nuclear HDAC4 protein than WT hT cells at basal conditions, but the amount of the protein was enhanced after dex only in AT cells. Nuclear HDAC4 phosphorylation status (Figure 1G), as observed by IF, showed

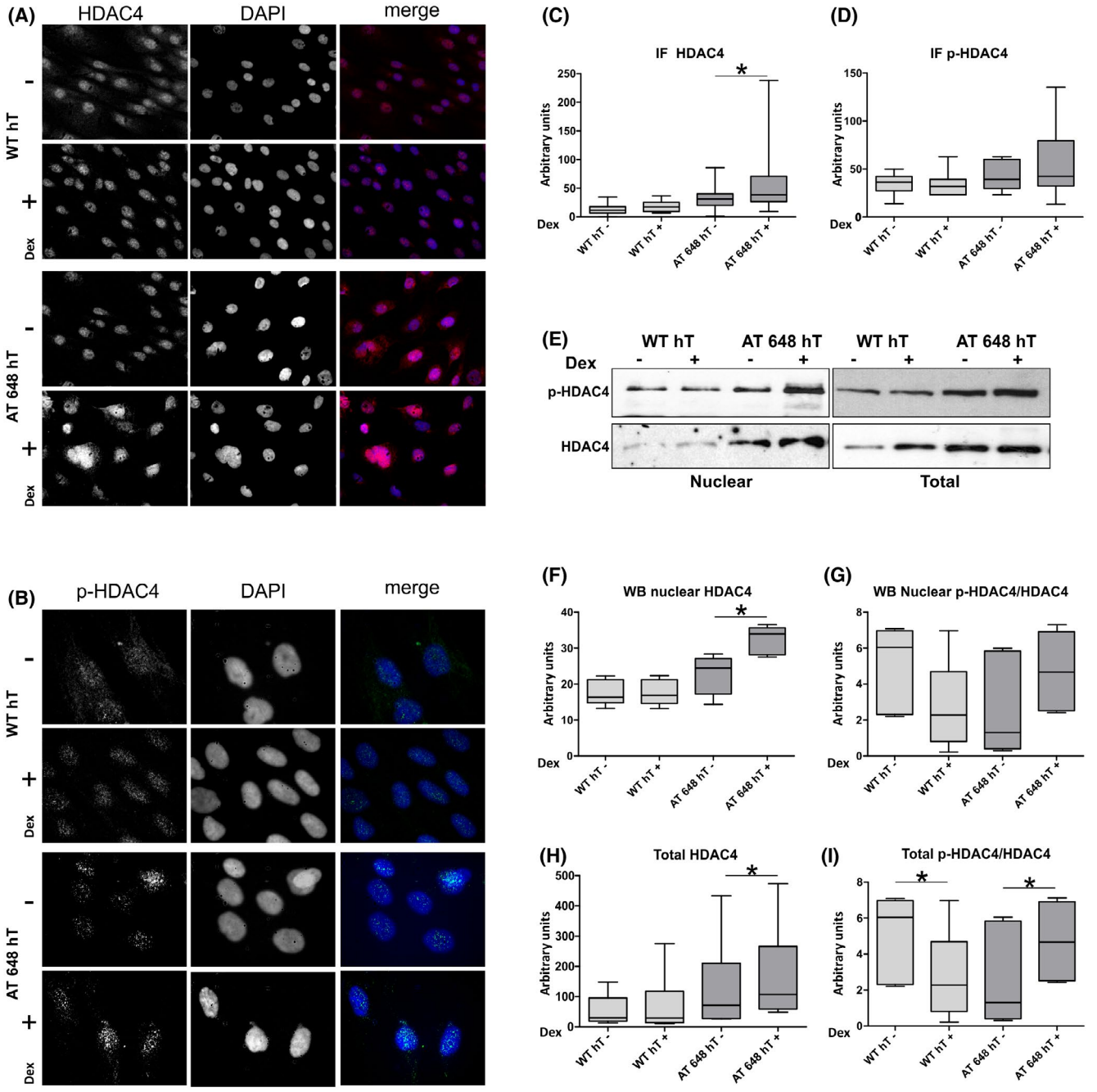

FIGURE 1 HDAC4 and p-HDAC4 are specifically modulated in AT cells by dex. A and B, Typical images illustrating the nuclear localization of HDAC4 and p-HDAC4 in control and dex-treated WT hT and AT 648 hT cells stained by IF. C and D, Quantification of the signals derived from the IF experiments. At least 200 nuclei were counted for data processing. HDAC4 only accumulated in AT 648 hT cells after dex treatment ($P = .012$ *t*-test), while no statistical differences were appreciable for p-HDAC4 quantitation. E-I, Western blot analysis on nuclear protein extracts and total protein extracts of all the tested cell lines. The quantitation of the immunoreactive bands is also reported. Nuclear HDAC4 only accumulated in AT 648 hT-treated cells (Wilcoxon test $P = .0313$ n = 9), while no differences were recorded for nuclear p-HDAC4. The analysis of total protein extracts showed an increment of HDAC4 in AT 648 hT-treated cells (Wilcoxon test $P = .313$ n = 9), while p-HDAC4 was downregulated in WT hT and upregulated in AT 648 hT-treated cells (Wilcoxon test $P = .0216$, n = 9)

a slight increase in nuclear p-HDAC4/HDAC4 only in the dex-treated AT 648 hT cell line, though the increase was not statistically significant. Western blot analyses of total protein extracts with the anti-HDAC4 antibody showed a significant increase in HDAC4 only in AT 648 hT cells (Figure 1H). Total phosphorylated HDAC4 was also tested and the ratio between pHDAC4/ HDAC4 showed an increase in treated AT 648 hT cells, while in WT hT cells, the ratio decreased after dex

treatment (Figure 1I). The increased HDAC4 phosphorylation status was in disagreement with its nuclear localization, since the phosphorylated protein should be shuttled to the cytosol.[33]

HDAC4 gene expression was also performed by qPCR assay, as illustrated in Supplemental Figure 1S. AT 648 hT cells showed an upregulation of HDAC4 gene expression after stimulation with dex compared to untreated AT 648 hT, whereas no significant differences were found between treated and untreated WT hT cells in terms of mRNA.

It is known that numerous posttranslational modifications regulate HDAC4 subcellular localization and activity, reviewed by Mielcarek et al,[46] Di Giorgio and Brancolini[47] and Wang et al.[48] In particular, the reduction of the disulfide bridge between cystein-667 and cystein-669, inhibits its nuclear export, in spite of its phosphorylation status.[43] Therefore, we investigated the possible activity of dex on HDAC4 redox status, and consequently whether HDAC4 nuclear accumulation was related to its reduced state. We evaluated HDAC4 redox status by BIAM assay, as described in the material and methods section.[42,43] As illustrated in Figure 2A,B, HDAC4 reduction was greatly increased only in treated AT 648 hT cells, whereas no significant differences were observed in WT hT cells.

As reported by Ago et al, in mice, thioredoxin (TXN) is able to regulate the localization of HDAC4, since the complex TXN-TBP-DNAJB5 reduces its disulfide bridge 667-669, promoting HDAC4 nuclear accumulation regardless of its phosphorylation status.

We then proceeded to investigate TXN gene expression by qPCR assay, as reported in Figure 3A. Higher mRNA expression levels of TXN were observed in both treated WT hT and AT 648 hT cell lines, suggesting that TXN overexpression may actually influence the nucleocytoplasmic shuttling of HDAC4 by cysteine reduction. Nuclear factor erythroid 2-related factor 2 (NFE2L2) is a key player in cellular redox balance, and the activation of NFE2L2 results in the induction of genes involved in oxidative stress protection, including TXN.[49,50] Since dex could enhance the cellular nuclear translocation of NFE2L2 in AT lymphoblastoid cell lines (LCLs),[27] NFE2L2 nuclear localization was investigated by western blotting analysis as shown in Figure 3B. Surprisingly, we were not able to record any nuclear shift in the tested cells. However, we did observe a higher nuclear amount of NFE2L2 in AT fibroblasts than WT.

The likelihood of HDAC4 nuclear accumulation by reduction is also supported by an autoregulatory feedback loop involving HDAC4 and miR-206.[51] HDAC4 in a reduced state suppresses miR-206 expression, thus avoiding the degradation of HDAC4 mRNA, a specific target of the previously mentioned miR. It has been shown through qPCR analysis that HDAC4 is overexpressed specifically in treated AT cells.

3.2 | HDAC4 does not influence HDAC3, MEF2A, and CREB

When situated in the nucleus, HDAC4 can play numerous roles, the first of which is the deacetylase function. For this activity, HDAC4 binds directly to HDAC3 in order to activate its deacetylase domain, becoming competent for epigenetic alterations.[52,53] To test nuclear HDAC4 deacetylase activity, we co-immunoprecipitated HDAC4 and then verified the presence of HDAC3 by western blotting using the anti-HDAC3 antibody, as reported in Supplemental Figure 2S. The interaction between HDAC4 and HDAC3 remained unaltered in AT 648 hT samples. In WT samples dex seemed to reduce HDAC4/HDAC3 binding.

Nuclear HDAC4 has an additional role in MEF2A and CREB activity suppression, promoting the downregulation

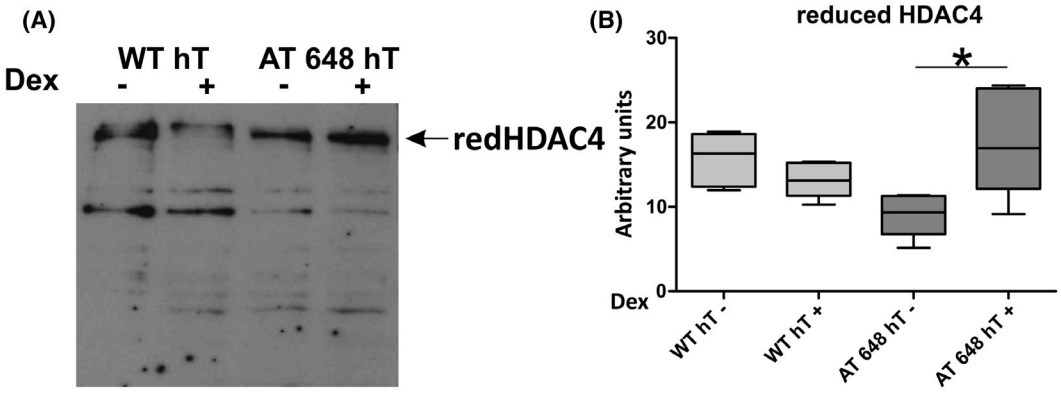

FIGURE 2 HDAC4 cysteins are reduced after dex treatment. A, Representative western blot image of the reduced HDAC4 immunoreactive bands obtained by biotin-modified cysteines captured by monomeric avidin beads and probed with anti-HDAC4 antibodies. B, Western Blot quantification. Dex improved the reduced status of HDAC4 only in AT 648 hT cells, promoting its nuclear translocation ($P = .0313$ Wilcoxon test, $n = 5$)

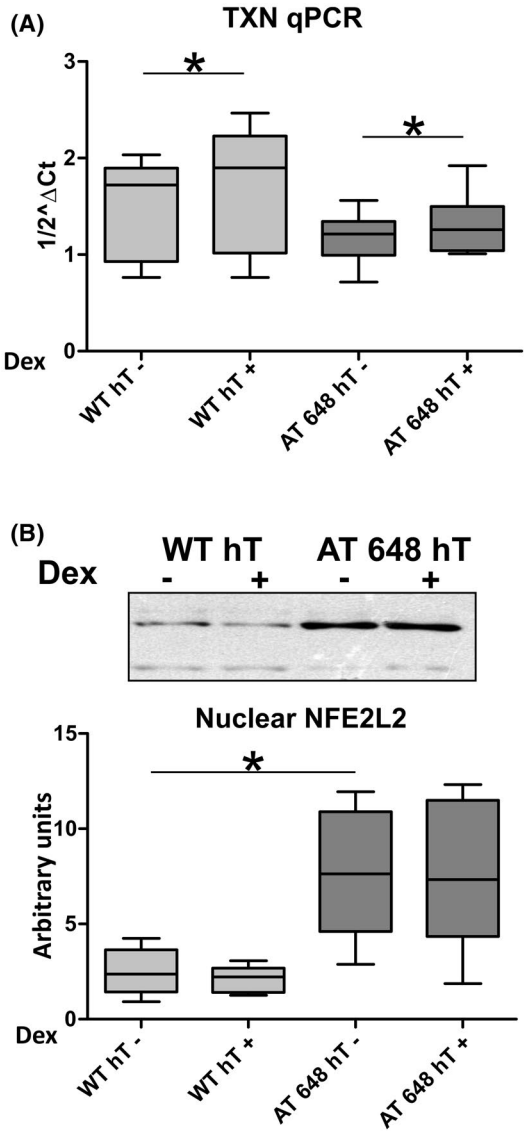

FIGURE 3 TXN is upregulated by dex in NFE2L2 in an independent manner. A, HDAC4 reduction should be mediated by TXN, which is actually overexpressed upon dex treatment in both WT hT and AT 648 hT cells (Wilcoxon test $P = .0239$ and $P = .041$, respectively, n = 5). B, The overexpression of TXN was not mediated by NFE2L2 since no further accumulation in the nucleus is observed after dex treatment in all the analyzed cell lines. However, a higher basal amount of nuclear NFE2L2 was observed in AT cells than in WT cells (Test U Mann-Whitney $P = .317$, n = 5)

of neuronal survival genes, leading to neurodegeneration in AT patients.[28] The activity of MEF2A and CREB in the investigated cells was therefore tested by a transcription factor (TF) array analysis, which also contained the assays for the above-mentioned TFs. MEF2A and CREB activity was undetectable in both AT 648 hT and WT hT fibroblasts, regardless of dex stimulation (Supplemental Figure 3S). However, among the TFs that were modulated in AT 648 hT by dex, the hypoxia inducible factor-1a (HIF-1a) was noted.

3.3 | Dex increases HIF1-a/HDAC4 interaction

HIF-1a is a heterodimer consisting of two subunits, oxygen-sensitive HIF-1a and constitutively expressed HIF-b. In hypoxic conditions, HIF-1a becomes stabilized, dimerizes with HIF-b and can translocate to the nucleus.[54] HIF-1a is involved in the modulation of numerous proteins and enzymes of glucose metabolism and the glycolytic pathway.[55] Tang et al[56] reported that HDAC4 has the ability to stabilize HIF-1a by 14.3.3ζ, promoting the expression of epithelial-mesenchymal transition (EMT or SLC22A1) transcription.

Since dex stimulates HIF-1a in AT 648 hT cells but not in WT hT cells, we focused our attention on whether HDAC4 nuclear accumulation could directly modulate HIF-1a activity in the proposed AT cellular model. Accordingly, the interaction between HIF-1a and HDAC4 was assayed by co-immunoprecipitation of HDAC4, and the immunocomplex was tested by western blotting with anti-HIF-1a and anti-14.3.3ζ/δ. Figure 4A shows the interaction enhancement in AT 648 hT cells after dex treatment between HIF-1a and HDAC4; only a weak signal was obtained in WT hT samples. The 14.3.3ζ interaction with HDAC4 was also assessed, and it seemed to decrease in AT cells after dex treatment. HIF-1a nuclear localization was performed on nuclear protein extracts as reported in Figure 4B, and a significant HIF-1a increase was observable in treated AT 648 hT cells, while we did not find significant differences between treated and untreated WT hT samples. The IF assay, with anti-HIF1a and anti-HDAC4 antibodies (Figure 4C) showed an HIF-1a fluorescent signal that was higher in dex stimulated AT 648 hT cells. A colocalization signal with HDAC4 was also observable in these cells.

The findings described above led us to investigate several HIF-1a downstream target genes, including SLC22A1, by qPCR, to assess their transcriptional activity. The expression of SLC22A1 was undetectable (in contrast with Tang et al[56]) in all the tested samples, while atypical outcomes were obtained testing the expression of vascular endothelial growth factor A (VEGFA), solute carrier family 2, facilitated glucose transporter member 1 (SLC2A1), insulin like growth factor-binding protein 1 (IGFBP-1), and glyceraldehyde-3-phosphate dehydrogenase (GAPDH) (Supplemental Figure 4S). Consequently, additional HIF-1a activities were investigated.

3.4 | HIF-1a/HDAC4 interaction bypasses ATM-dependent DDIT4 transcription

Cam et al[11] reported that ATM is able to phosphorylate HIF-1a in Ser696 in hypoxic conditions, driving DDIT4

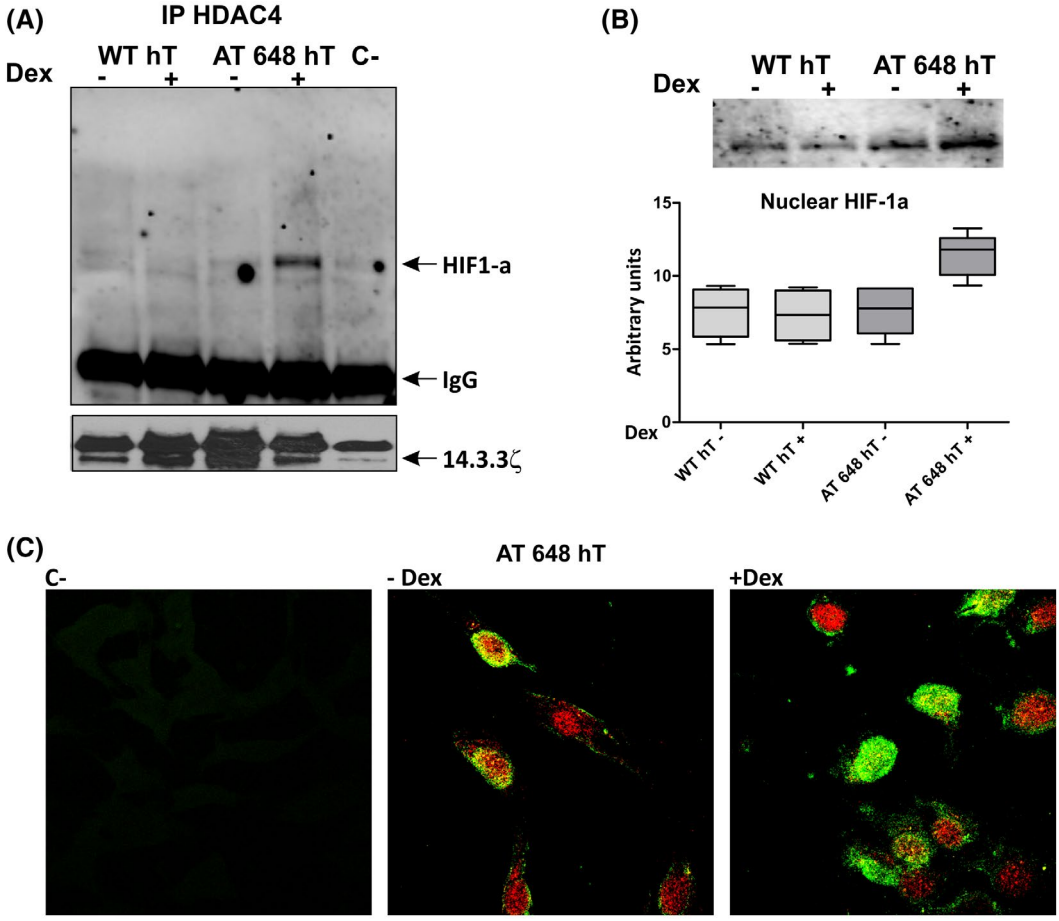

FIGURE 4 HDAC4 interaction with HIF-1a is boosted after dex treatment. A, Representative western blot of HIF-1a and 14.3.3 ζ/δ probed membranes containing HDAC4 co-immunoprecipitated proteins. Dex enhanced HDAC4-HIF-1a interaction in AT 648 hT cells. Weak signals were observed in other lanes. Dex seemed to reduce the HDAC4-14.3.3 ζ interaction in AT 648 hT cells. B, Representative western blot analysis of the HIF-1a nuclear amount from all cell line conditions. Quantitation is also reported and HIF-1a only accumulated in AT 648 hT cells after dex stimulation (Wilcoxon test $P < .0313$ n = 7). C. HIF-1a nuclear localization (green) was also observed by indirect immunofluorescence imaging of AT cells treated with dex or untreated, and in some loci it colocalizes with HDAC4 (red)

(also known as REDD1) expression in AT mouse embryonic fibroblasts (MEFs) and in human AT fibroblasts. DDIT4 in turn, indirectly leads to the suppression of the mammalian target of rapamycin (mTORC1),[57] therefore improving the autophagy process, one of the compromised biological pathways in AT cells.[58] This prompted us to assess whether dex might somehow modulate HIF-1a by HDAC4, bypassing the HIF-1a phosphorylation by ATM, and controlling the HIF-1a-mediated DDIT4 transcription. We therefore first assessed DDIT4 mRNA expression and protein levels after dex treatment by qPCR and western blotting, using the anti-DDIT4 antibody as shown in Figure 5A,B, respectively. The DDIT4 transcript was found to be significantly overexpressed only in treated AT 648 hT, whereas no significant changes were observed in WT hT. In contrast, the DDIT4 protein showed a slight increase in WT hT cells after dex treatment, but showed its largest increase in AT 648 hT cells treated with dex.

Once it had been established that DDIT4 expression is influenced by dex action, we turned our attention to the possible HIF-1a/HDAC4 interaction in the HIF-1a-binding site localized in the DDIT4 promoter.[59]

First, we performed a gel shift assay using a probe surrounding the HIF-1a-binding site. As reported in Supplemental Figure 5S, at least three protein-DNA complexes were observable in all conditions. The super-shift by HDAC4 or HDAC4 and HIF-1a antibodies seemed to affect the composition of the complexes, especially in the treated AT 648 hT sample. In order to obtain further confirmation of the gel shift results, the immunoprecipitation of chromatin (ChIP) on AT 648 hT cells was achieved with HDAC4 and HIF-1a antibodies. The fragments surrounding the DDIT4 promoter HIF-1a-binding site were quantified by qPCR. As shown in Figure 6A, there was no significant difference between treated and untreated AT 648 hT in terms of the amount of HIF-1a in the DDIT4 promoter,

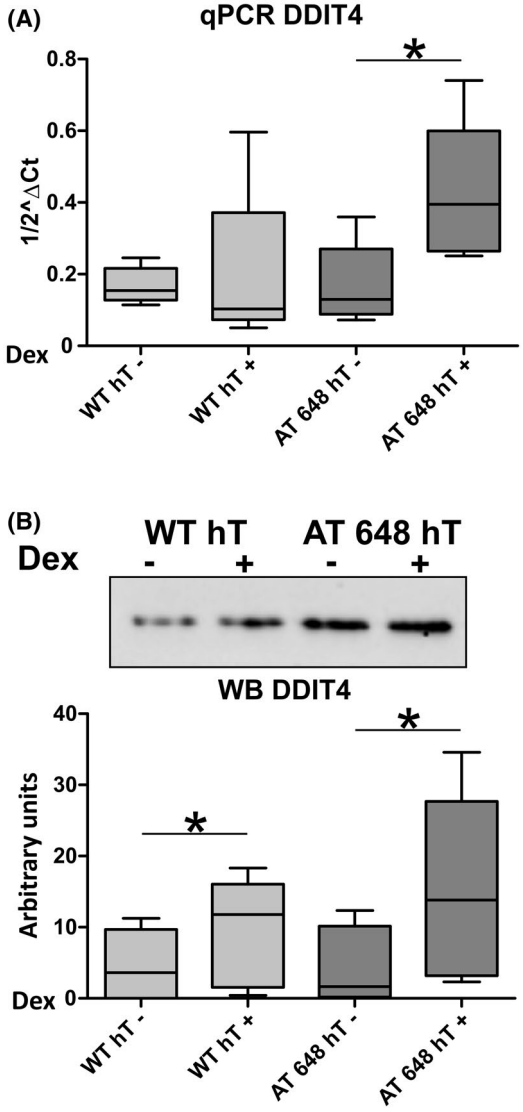

FIGURE 5 DDIT4 gene expression is specifically induced by dex in AT. A, Analysis by qPCR shows that dex specifically modulates the DDIT4 transcript only in AT 648 hT-treated cells (Wilcoxon test $P = .0313$ n = 7). B, Representative western blot and matching quantification of DDIT4 in total protein extracts. A DDIT4 protein boost was evident in treated AT 648 hT (Wilcoxon test $P = .0355$ n = 6). At the protein level, a small increment was also observable in WT hT dex-treated cells (Wilcoxon test $P = .035$ n = 6)

while qPCR on anti-HDAC4 ChIP showed a larger amount of HDAC4 in the same promoter locus in dex treated AT 648 hT cells.

DDIT4 transcription dependence on HIF-1a/HDAC4 was assayed by gene silencing experiments and DDIT4 expression was evaluated. In both HIF-1a and HDAC4 silencing, we observed a reduction in the amount of transcript (a downregulation of about 50%-60%, Figures 6B,C, respectively) only in AT 648 hT cells. In fact, in all WT hT conditions and in untreated AT 648 hT cells, the mRNA levels remained unaffected by siRNA treatments, thus reinforcing the idea that HDAC4 is responsible for HIF-1a DDIT4 transcription. In silencing experiments, the DDIT4 protein amount was also evaluated as reported in Figure 6D (quantified in Supplemental Figure 6SA), and its expression matched the mRNA amount. Additional results, including HIF-1a downregulation in siRNA experiments and the relationship between the amount of HIF-1a and DDIT4 expression, are reported in Supplemental Figure 6SB and C, respectively.

Taken together, these findings show that DDIT4 is actually transcribed by the HIF-1a-HDAC4 complex after dex induction, bypassing ATM activity selectively in AT cells.

3.5 | Autophagy is enhanced by dex without mTORC1 activation

DDIT4 can activate the TSC1/2 complex, which converts Rheb to the inactive GDP-bound state, leading to the inhibition of mTORC1 activity[60] and indirectly promoting autophagy.[61,62]

Autophagy dysfunctions are involved in several neurodegenerative diseases[63] and these impairments have also been described in AT.[58] Since the above-mentioned results concern DDIT4 increase, we decided to investigate the autophagy pathway in dex-treated AT cells. To detect autophagic flux, microtubule-associated protein light chain 3 (LC3) was assayed as an autophagy marker. During autophagy, the cytoplasmic form LC3-I is recruited to autophagosomes and converted to LC3-II through lipidation, and LC3-II associates with autophagosomal membranes. The amount of the lipidated form LC3-II is correlated with the number of autophagosomes.[64,65] Considering that LC3B-II is rapidly degraded inside autolysosomes, LC3 immunoblotting may not reflect the real autophagy activation.[66-68] Hence, to investigate the accurate autophagic flux, we performed LC3B degradation blocking experiments (Figure 7A). In basal conditions, without inhibitor treatment, the level of LC3B-II decreased in both dex-treated WT and AT cells, although the reduction was more evident in AT samples. Under chloroquine treatment, AT 648 hT showed an increase in LC3B-II, whereas WT cells exhibited a decrease after dex treatment, but both outcomes were not statistically significant. In the chloroquine plus pepstatin condition, no differences were observable in WT hT cells, while a statistically significant LC3B-II accumulation was detected in dex-treated AT 648 hT samples. To monitor autophagic flux, in addition to LC3B, the p62 (SQSTM1/sequestosome 1) marker was also tested. Its degradation reflects an enhancement of the autophagic process. p62-Ubiquitin and LC3B are associated with mature autophagosomes and then degraded into autolysosomes.[69] The p62 protein level was assayed on total protein extracts via western blot analysis with anti-p62 antibody. Figure 7B shows a significant decrease in p62 in AT-treated cells. On the other hand, no

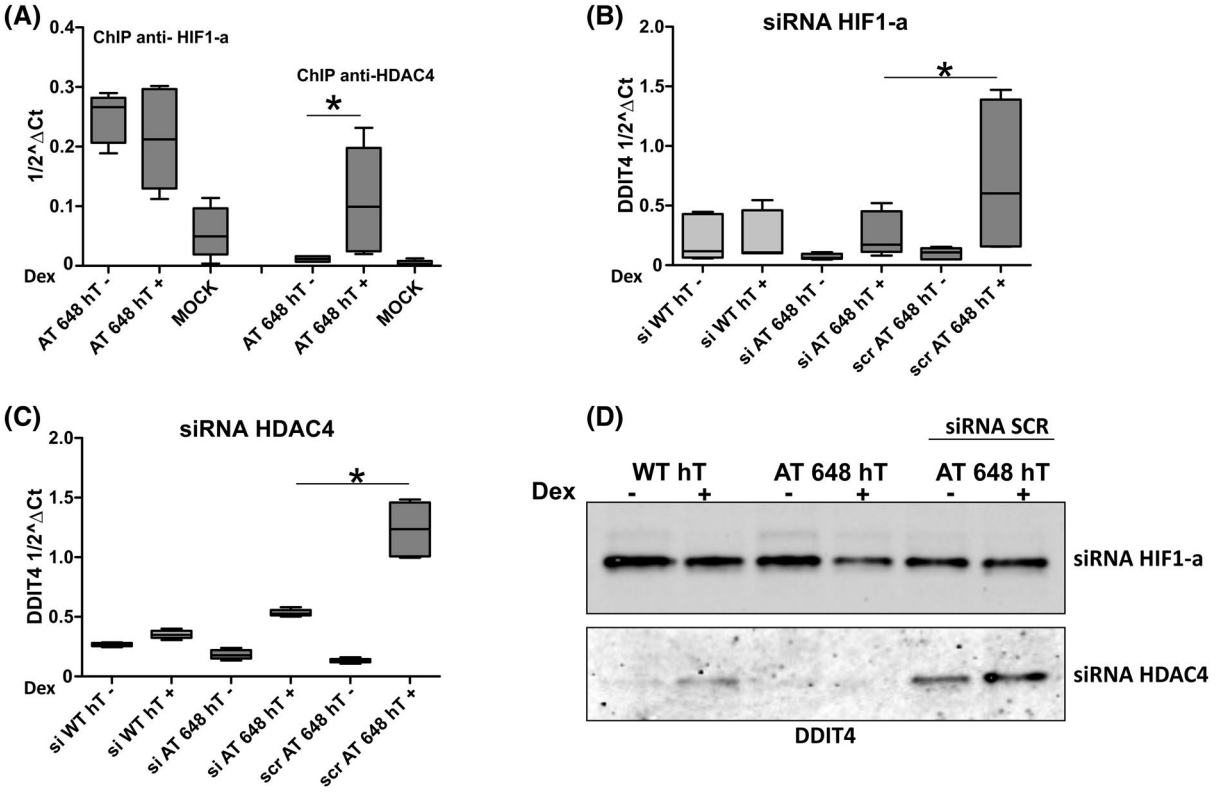

FIGURE 6 DDIT4 is selectively transcribed in AT cells by the HIF-1a-HDAC4 complex after dex stimulation. A, qPCR quantification of ChIP outcome in AT 468 hT cells revealed that the amount of HIF-1a in the DDIT4 promoter was unaltered (Wilcoxon test $P = .14$, n = 5), while the amount of HDAC4 was markedly increased after dex treatment (Wilcoxon test $P = .0355$, n = 5). B-C, The silencing of HIF-1a and HDAC4 by siRNAs, decreased DDIT4 expression in treated AT 648 hT cells by approximately 70% (siRNA HIF-1a, Wilcoxon test $P = .0313$ n = 7) and by approximately 50% (siRNA HDAC4, Wilcoxon test $P = .0084$ n = 6) when compared to the siRNA SCR dex-treated control. No differences between siRNA SCR and siRNA HIF-1a or siRNA HDAC4-untreated AT cells were observed. DDIT4 transcription is improved by HDAC4 HIF-1a stabilization upon dex stimulation specifically in AT cells. D. DDIT4 protein amounts in HIF-1a and HDAC4 targeting siRNAs in all the tested cell lines. DDIT4 protein levels were also reduced in treated AT 648 hT after HIF-1a and HDAC4 silencing. DDIT4 HIF-1a-silenced western blot quantification is reported in Supplemental Figure S6

significant difference was observed in the WT hT sample. Finally, the VPS18 autophagy marker was also evaluated. VPS18 is a central subunit of the VPS-C core complex involved in fusion between endosomes and lysosomes or autophagosomes and lysosomes.[70,71] VPS18 is critical for autophagosome clearance.[72] VPS18 protein level was assessed using anti-VPS18 and the quantifications are illustrated in Figure 7C. The amount of VPS18 protein decreased in AT 648 hT after dex treatment bringing VPS18 to the same levels as those found in WT hT cells, which were unaffected by dex stimulation. The VPS18 gene expression was detected by qPCR (Supplemental Figure 7S). VPS18 mRNA content was increased in AT-treated cells, while there was not a significant difference in the WT hT sample. The results for LC3B, p62, and VPS18 support the positive dex-induced effects on autophagic flux in AT fibroblasts.

DDIT4 should stimulate autophagy by acting indirectly on mTORC1 complex, which is an atypical serine/threonine protein kinase. mTORC1 is the master regulator of cell growth and coordinates the cellular response to growth factors and nutrient sufficiency.[73] The main downstream targets of mTORC1, p70 ribosomal protein S6 kinase (p70S6K), and eukaryotic translation initiation factor 4E (eIF4E)-binding protein 1 (4E-BP1), are involved in the translation initiation process.[74] Therefore, the activity of mTORC1 was investigated by testing p70S6K and 4E-BP1 phosphorylation. We expected a decreased phosphorylation of both targets in AT cells treated with dex, but surprisingly no significant differences among the samples were observed (Supplemental Figure 8S). This unexpected outcome led us to test the effects of dex on HIF-1a-silenced fibroblasts. In Figure 8, p-p70S6K normalized signal is reported. Only in dex-stimulated AT 648 hT we observed a large amount of phosphorylated p70S6K, while no differences were observed in p-4E-BP1.

This behavior could be due to the mTORC1 activation in AT cells after dex treatment, since its upstream pathway was found to be activated, as reported in Figure 9A. Dex induced AKT phosphorylation, especially in AT 648 hT cells, which

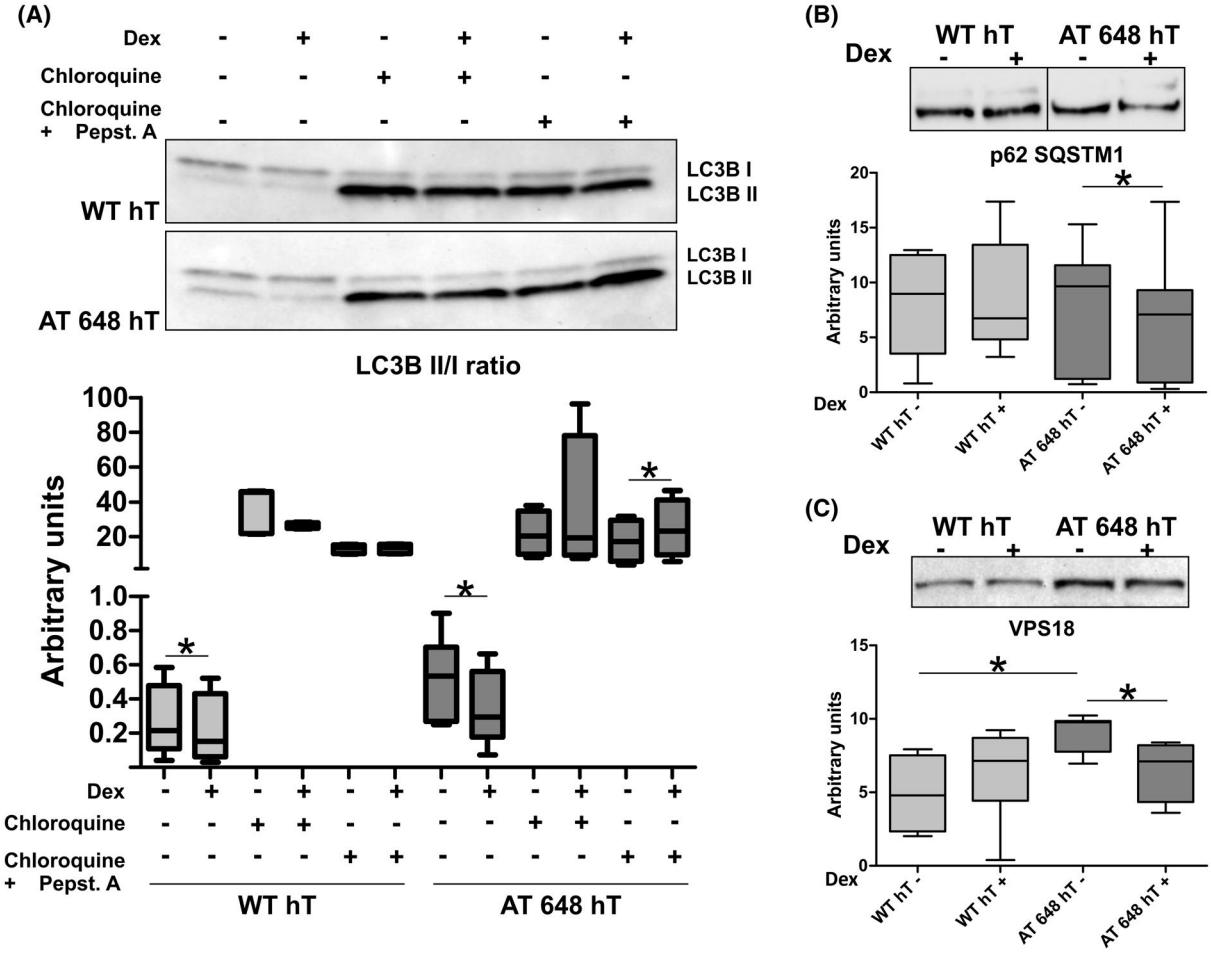

FIGURE 7 Autophagy is specifically improved in dex-treated AT cells. A, Representative western blot of total protein extracts of the LC3-I and LC3-II immunoreactive bands of all the experimental conditions after 4 hour of treatment with chloroquine and chloroquine plus pepstatin A. The western blot quantification shows the LC3-II/LC3-I ratio. The increased LC3 II/I ratio after chloroquine-pepstatin A was only detected in treated AT 648 hT, suggesting an autophagic flux improvement (Wilcoxon test $P = .138$ n = 8). A slight decrement of LC3 II/I ratio was observed both in unblocked WT hT and AT 648 hT treated with dex (Wilcoxon test $P = .0345$ n = 8 and $P = .035$ n = 8, respectively). B, p62/SQSTM1 western blot and quantification of total protein extracts of all the tested cell lines. The p62 downregulation confirmed the enhancement of the autophagic flux in AT 648 hT after dex stimulation. WT hT did not show any significant differences in terms of p62 content. (Wilcoxon test $P = .026$ n = 8). C, Western blot quantification of VPS18 of whole protein extracts of all the tested cell lines. AT cells showed a higher basal amount of the VPS18 protein than the WT cells (Mann-Whitney U test $P = .0038$ n = 7), suggesting an impairment of the autophagosome-lysosome fusion. Dex decreased and restored the amount of the VSP18 protein in AT 648 hT bringing its level to that of the WT hT protein (Wilcoxon test $P = .0140$ n = 7)

also showed increased p-GSKb levels (Figure 9B). The AKT signaling in AT cells should promote mTORC1 activation, but the simultaneous DDIT4 expression counteracts this stimulation at the mTORC1 level.

3.6 | Inferring HDAC4 and DDIT4 expression in AT patients

We have previously described the blood gene expression variation in AT patients enrolled in the EryDex clinical trial (IEDAT EudraCT Number 2010-022315-19),[16] in healthy subjects and in untreated AT patients by microarray analysis.[21]

Among the differentially expressed probes in patients who received the treatment and the untreated subjects, we observed an expression increment in HDAC4 and DDIT4 genes. These indications were validated in the present investigation by qPCR, confirming that HDAC4 and DDIT4 gene expression is modulated in AT patients receiving dex (Figure 10A,B, respectively). HDAC4 expression was found to be statistically different in all three tested groups. This means that dex can improve HDAC4 expression deficiency in AT patients raising it to levels found in healthy subjects. DDIT4 was found to be statistically downregulated in AT patients compared to healthy subjects. Dex improved DDIT4 expression in EryDex AT patients, but not in all subjects ($P = .1$).

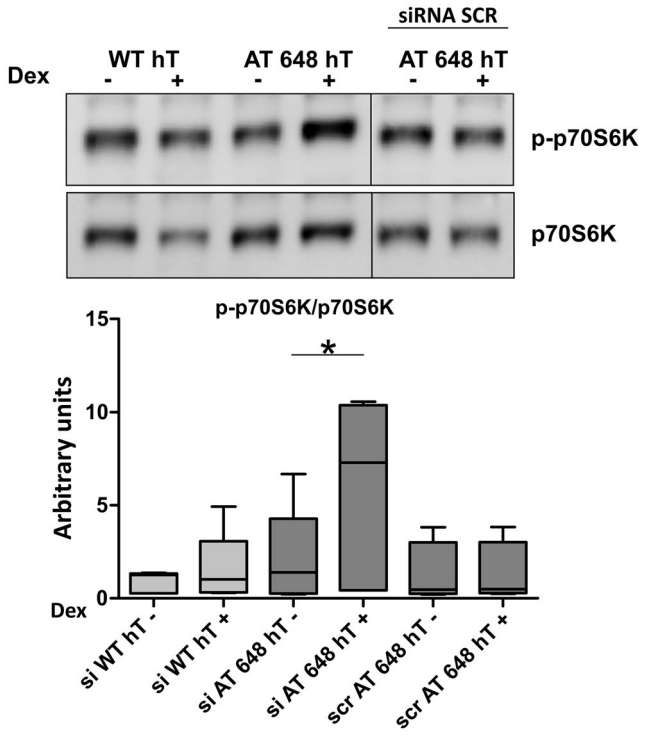

FIGURE 8 p-p70S6K is activated in treated HIF-1a-silenced AT cells. p-p70S6K and p70S6K representative western blots of HIF-1a-silenced WT hT and AT 648 hT cells and corresponding quantification. The silenced dex-treated AT 648 hT sample showed a high phosphorylation of p70S6K (Wilcoxon test $P = .0313$ n = 6)

4 | DISCUSSION

Ataxia Teleangiectasia is a severe syndrome, and no effective disease-modifying treatment is available. Only supporting therapies are used to care for patients. However, in the last few years, observational studies and clinical trials have shown that treatment with glucocorticoids improves symptoms and neurologic functions in patients with AT. The authors of the present study have previously described the influence of dex in AT patients and in LCLs.

Since the lack of ATM leads to HDAC4-induced neurodegeneration,[28] we assessed whether dex could reverse this state by re-locating HDAC4 in cells. Our findings have led us to propose a new molecular mechanism for the nonepigenetic regulation of gene expression by HDAC4. In contrast to previously published data by Li et al reporting that nuclear HDAC4 promoted neurodegeneration, we suggest a different role for HDAC4, which was found to act as a direct transcription regulator in AT fibroblasts, leading to an unexpected outcome.

Our initial results showed an extra nuclear HDAC4 accumulation in AT cells after dex treatment, by cysteine reduction and not by phosphosignaling. Since this observation of such a dex effect in AT cells was unexpected, we decided to investigate this event thoroughly. The clinical data of patients treated with dex[16,17,21,36] actually showed an improved neurological outcome, and it was hard to consider the HDAC4 nuclear shift as a side effect. In fact, the

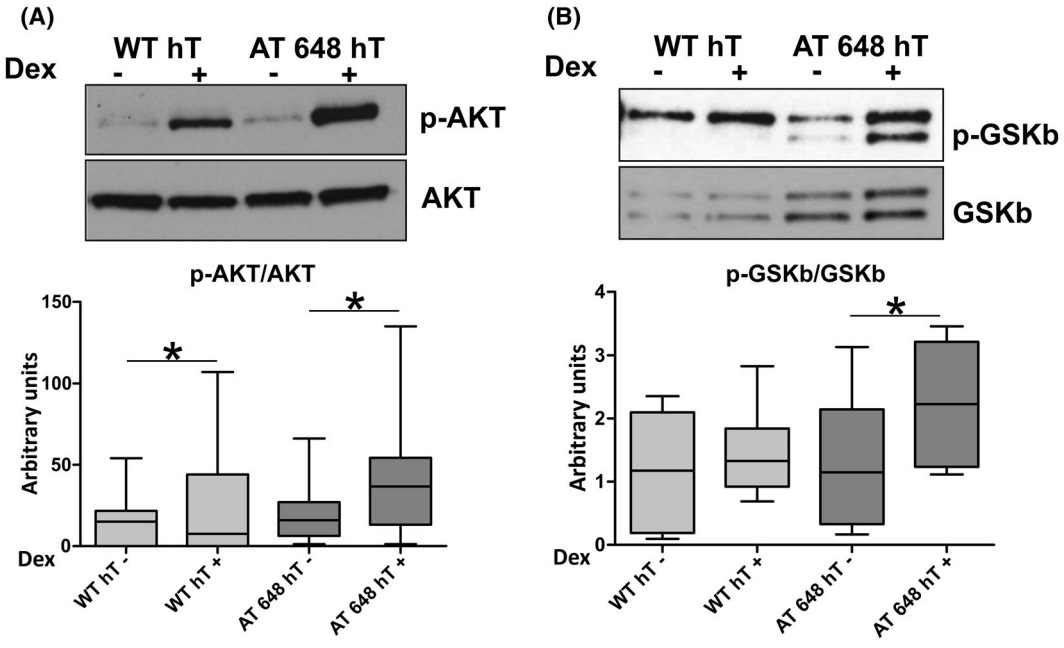

FIGURE 9 Dex stimulates upstream activator of mTORC1. A, Western blot representation of p-AKT and AKT and quantification of p-AKT/AKT ratio in WT hT and AT 648 hT cells. Dex induced AKT phosphorylation, especially in AT 648 hT cells and to a lesser extent in WT hT cells (Wilcoxon test $P = .009$ and $P = .031$, respectively, n = 13). B, Western blot image of p-GSKb and GSKb and quantification of p-GSKb/GSKb ratio of all tested cells with or without dex. GSKb is more phosphorylated only in the treated AT 648 hT sample (Wilcoxon test $P = .0156$ n = 8)

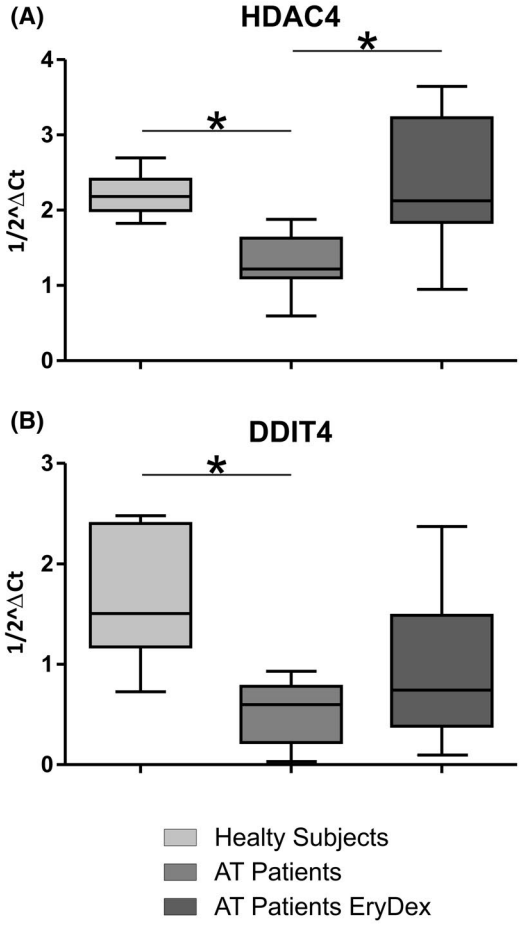

FIGURE 10 HDAC4 and DDIT4 are also modulated by dex in AT patients. A, HDAC4 qPCR on patients' samples, previously tested by microarray analyses, revealed that HDAC4 is downregulated in AT patients compared to healthy subjects, and the gene expression in AT patients who received EryDex was restored (Kruskal-Wallis $P = .036$ followed by Dunn test). B, Like HDAC4, DDIT4 was downregulated in AT patients compared to healthy subjects (Kruskal-Wallis $P = .016$ followed by Dunn test), and dex improved DDIT4 mRNA levels only in some treated patients

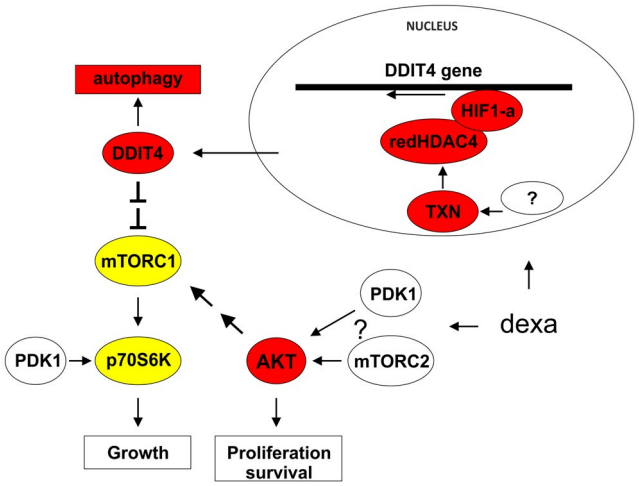

FIGURE 11 Hypothesized Biomolecular pathway induced by dex in AT. Schematic representation of the probable pathways that regulate autophagy and proliferation selectively modulated by dex treatment in AT cells. Only treated AT cells showed a biological switch: the proliferation and survival pathways are predominant over the growing pathway. Autophagic improvement can sustain this switch

findings reported in the present paper are not in agreement with those reported in literature. First, the accumulation by cysteine reduction should be TXN mediated,[43,51] and our results showed a dex-dependent increment of TXN expression, but unlike previously published data, concerning AT LCLs,[27] this overexpression seemed to be NFE2L2 independent. Second, cysteine mediated nuclear localization of HDAC4 is not related to its deacetylase activity, as the interaction with the HDAC3 protein remained unaltered in AT after dex treatment. Hence, redHDAC4 probably has some other functions. Third, the effect of HDAC4 on the transcription factors MEF2A and CREB was not observable in the proposed fibroblasts; thus, their repression by HDAC4 was unquantifiable.

Several other transcription factors were dex modulated in the TF array experiments. Among these, HIF-1a was selected as a potential partner of HDAC4, and this interaction was investigated. Actually, dex is capable of selectively increasing the interaction between HIF-1a and HDAC4 only in AT cells, and its nuclear amount was increased. The described interaction is able to stabilize HIF-1a transcription activity,[56] but the described gene modulation (SLC22A1) was not evident in AT fibroblasts. In addition, a panel of classical genes regulated by HIF-1a was evaluated, but the results were unusual and contradictory. The HIF-1a pathway analysis led us to investigate the possibility that HDAC4 HIF-1a interaction might be able to modulate DDIT4 expression bypassing ATM activation, which is responsible for inducing HIF-1a activity in hypoxia conditions. Obviously, we were not interested in hypoxia conditions, but simply in testing whether the axis dex-HDAC4-HIF-1a and DDIT4 could activate and restore autophagy, a compromised molecular mechanism in AT cells.[58] It is known that dex induces DDIT4 in some cells such as lymphocytes[62] and thymocytes,[75] in rat skeletal muscle[76] and rat hippocampus.[77] However, in the above-mentioned papers, the administered dex was in the micromolar concentration range, and the overexpression disappeared after 24-36 hours depending on the cell type. In contrast, our data showed an increase in DDIT4 mRNA and protein amounts only in AT fibroblasts, while WT cells were unaffected. Furthermore, the induction was present at nanomolar dex concentrations, and DDIT4 expression was protracted until 72 hours. Moreover, the molecular mechanism of action of DDIT4 induced by dex in all the investigated cell lines was unknown. The present paper illustrates for the first time a likely mechanism of

action through which dex can modulate DDIT4 expression, although this mechanism seems to be limited to AT cells. Indeed, the HIF-1a stabilization and activity by HDAC4 on the DDIT4 gene was observable only in AT cells and not in WT samples. The induction of DDIT4 represented a very important pathway, since it is involved in the autophagy process that was restored after dex administration as reported in the results section. In addition, the utilized AT fibroblasts showed vesicle fusion impairment as documented by D'Assante et al. Actually, the amount of VPS18 messenger was lower in AT than in WT samples at the basal condition.[58] Furthermore, the analysis of VPS18 protein, markedly higher in AT untreated samples, suggested a large amount of CORVET and HOPS tethering complexes in the cells. This may be due to the large amount of vesicles/autophagosomes that are not able to correctly fuse to lysosomes. The LC3B-II analyses confirm an improvement in autophagic flux in AT cells and further reinforce the idea that the problem in the AT autophagy process is the fusion between autophagosomes and lysosomes, since the LC3B-II/I ratio is statistically boosted in chloroquine-pepstatin A experiments.[68] Dex treatment of AT cells reinstated the levels of VPS18 protein to levels found in WT and the mRNA level was also restored, which is consistent with the improved autophagic flux. Finally, p62 levels confirmed the enhancement of autophagy.

Since autophagy is typically tuned by the mTORC1/DDIT4 pathway, we decided to test the mTORC1 activity, which should have been downregulated. The mTORC1 targets were assayed, but they were inexplicably unaffected after dex administration, and thus unaffected by DDIT4 overexpression. At this point, we wondered if some other signaling was activated upstream. To this aim, we investigated the activity of mTORC1 when the axis HIF-1a-DDIT4 was switched off. Surprisingly, p70S6K was found to be activated in only silenced treated AT samples, leading us to hypothesize that dex might exert an upstream activation of mTORC1 in AT, probably through the AKT signaling, which was strongly activated and its pathway sustained GSKb phosphorylation in AT. We therefore suggest that DDIT4 may counteract mTORC1-dependent AKT stimulation. AKT in turn can be regulated by PDK1[78,79] or by the mTORC2 complex.[80] PDK1 can also directly act on p70S6K,[78] which was always found to be unaffected by dex action in the tested cells; thus, we can assume that AKT phosphorylation is mediated by mTORC2.

How dex can stimulate AKT signaling through the above-mentioned mechanisms remains unclear, even though a short-term glucocorticoid nongenomic pathway was described by Matthews et al.[81] The authors described a dexamethasone AKT activation lasting only a few minutes after treatment; on the contrary, we observed this event for at least 4 days treatment (also noted in another type of AT cells).[22]

In light of all of these findings, we can propose that, only in AT-treated cells, there is a signaling branching through which the growing signaling (AKT-mTORC1-p70S6K), reviewed by Jewell and Guan[82] and by Saxton and Sabatini,[83] is switched to survival and proliferation signaling (AKT-GSKb).[84,85]

At this point, the described autophagic flux improvement after dex treatment seems to be mTORC1 independent, but the mechanisms of its activation should be further investigated. In any case, we can hypothesize that an additional DDIT4 function can also be exerted in AT cells in the same manner that it can be exerted in human osteosarcoma cells and mouse embryo fibroblasts, as proposed by Qiao et al. In fact, DDIT4 can also control autophagosome-lysosome fusion by inhibiting ATG4b-mediated LC3-II delipidation to LC3-I.[61] Lipidated LC3B is essential for the correct movement forward of lysosomes and a proper fusion.[86] This possible DDIT4 activity through dex in the reported cellular model is in agreement with confirmed findings that the impairment of autophagic flux in AT is due to autophagosome-lysosome fusion deficiency. Nevertheless, the slight autophagy enhancement can endure the described DDIT4-AKT-mediated survival and proliferation signaling from an energy balance standpoint. Based on all of the findings described above, the proposed signaling that occurs specifically in AT fibroblasts treated with dex is shown in Figure 11. Finally, the availability of AT patients' data led us to explore the possibility that the aforementioned biological pathway may occur in dex-treated subjects. Indeed, HDAC4 was found to be statistically altered in AT patients compared to healthy subjects, and dex changed this state. DDIT4 varied between healthy and AT subjects; some, but not all patients treated with dex improved their DDIT4 gene expression level. The number of analyzed patients is critical for the correct outcome estimation and the patient's genetic variability might contribute to their response to dex. It could be interesting to extend these gene expression variations in an ongoing phase III clinical trial (EDAT-02-2015 NCT02770807). It has to be noted that in the last few years, DDIT4 has been incongruously described as being involved in several types of malignancies and cancer therapy.[87] In light of the findings reported here and the fact that AT patients are particularly prone to tumor development, we propose that the DDIT4 pathway should be carefully evaluated and further investigated for the thorough treatment of these patients.

ACKNOWLEDGMENTS

This study was partially supported by FanoAteneo and by EU H2020 IEDAT (Grant n°: 667946).

CONFLICT OF INTEREST

Mauro Magnani holds stock ownership in EryDel S.p.A. None of the authors have competing interests.

AUTHOR CONTRIBUTIONS

Anastasia Ricci and Michele Menotta were responsible for the experimental design, the execution of the experiments, data collection, and interpretation and the writing of the paper. Luca Galluzzi contributed to the experimental design and edited the paper. Mauro Magnani contributed to the revision of the paper and financial support.

REFERENCES

1. Gatti RA, Berkel I, Boder E, et al. Localization of an ataxia-telangiectasia gene to chromosome 11q22-23. *Nature*. 1988;336:577-580.
2. Abraham RT. PI 3-kinase related kinases: 'big' players in stress-induced signaling pathways. *DNA Repair*. 2004;3:883-887.
3. Chun HH, Gatti RA. Ataxia-telangiectasia, an evolving phenotype. *DNA Repair*. 2004;3:1187-1196.
4. Gilad S, Chessa L, Khosravi R, et al. Genotype-phenotype relationships in ataxia-telangiectasia and variants. *Am J Hum Genet*. 1998;62:551-561.
5. Lavin MF. Ataxia-telangiectasia: from a rare disorder to a paradigm for cell signalling and cancer. *Nat Rev Mol Cell Biol*. 2008;9:759-769.
6. Biton S, Barzilai A, Shiloh Y. The neurological phenotype of ataxia-telangiectasia: solving a persistent puzzle. *DNA Repair*. 2008;7:1028-1038.
7. Bakkenist CJ, Kastan MB. DNA damage activates ATM through intermolecular autophosphorylation and dimer dissociation. *Nature*. 2003;421:499-506.
8. Kozlov SV, Graham ME, Peng C, Chen P, Robinson PJ, Lavin MF. Involvement of novel autophosphorylation sites in ATM activation. *EMBO J*. 2006;25:3504-3514.
9. Abraham RT. Cell cycle checkpoint signaling through the ATM and ATR kinases. *Genes Dev*. 2001;15:2177-2196.
10. Guo Z, Kozlov S, Lavin MF, Person MD, Paull TT. ATM activation by oxidative stress. *Science*. 2010;330:517-521.
11. Cam H, Easton JB, High A, Houghton PJ. mTORC1 signaling under hypoxic conditions is controlled by ATM-dependent phosphorylation of HIF-1alpha. *Mol Cell*. 2010;40:509-520.
12. Yang DQ, Kastan MB. Participation of ATM in insulin signalling through phosphorylation of eIF-4E-binding protein 1. *Nat Cell Biol*. 2000;2:893-898.
13. Sharma NK, Lebedeva M, Thomas T, et al. Intrinsic mitochondrial DNA repair defects in Ataxia Telangiectasia. *DNA Repair*. 2014;13:22-31.
14. Alexander A, Cai SL, Kim J, et al. ATM signals to TSC2 in the cytoplasm to regulate mTORC1 in response to ROS. *Proc Natl Acad Sci USA*. 2010;107:4153-4158.
15. Alexander A, Kim J, Walker CL. ATM engages the TSC2/mTORC1 signaling node to regulate autophagy. *Autophagy*. 2010;6:672-673.
16. Chessa L, Leuzzi V, Plebani A, et al. Intra-erythrocyte infusion of dexamethasone reduces neurological symptoms in ataxia teleangiectasia patients: results of a phase 2 trial. *Orphanet J Rare Dis*. 2014;9:5.
17. Leuzzi V, Micheli R, D'Agnano D, et al. Positive effect of erythrocyte-delivered dexamethasone in ataxia-telangiectasia. *Neurol Neuroimmunol Neuroinflamm*. 2015;2:e98.
18. Buoni S, Zannolli R, Sorrentino L, Fois A. Betamethasone and improvement of neurological symptoms in ataxia-telangiectasia. *Arch Neurol*. 2006;63:1479-1482.
19. Zannolli R, Buoni S, Betti G, et al. A randomized trial of oral betamethasone to reduce ataxia symptoms in ataxia telangiectasia. *Mov Disord*. 2012;27:1312-1316.
20. Broccoletti T, Del Giudice E, Amorosi S, et al. Steroid-induced improvement of neurological signs in ataxia-telangiectasia patients. *Eur J Neurol*. 2008;15:223-228.
21. Menotta M, Biagiotti S, Orazi S, et al. In vivo effects of dexamethasone on blood gene expression in ataxia telangiectasia. *Mol Cell Biochem*. 2018;438:153-166.
22. Menotta M, Biagiotti S, Bianchi M, Chessa L, Magnani M. Dexamethasone partially rescues ataxia telangiectasia-mutated (ATM) deficiency in ataxia telangiectasia by promoting a shortened protein variant retaining kinase activity. *J Biol Chem*. 2012;287:41352-41363.
23. Broccoletti T, Del Giudice E, Cirillo E, et al. Efficacy of very-low-dose betamethasone on neurological symptoms in ataxia-telangiectasia. *Eur J Neurol*. 2011;18:564-570.
24. Cirillo E, Del Giudice E, Micheli R, et al. Minimum effective betamethasone dosage on the neurological phenotype in patients with ataxia-telangiectasia: a multicenter observer-blind study. *Eur J Neurol*. 2018;25:833-840.
25. Russo I, Cosentino C, Del Giudice E, et al. In ataxia-teleangiectasia betamethasone response is inversely correlated to cerebellar atrophy and directly to antioxidative capacity. *Eur J Neurol*. 2009;16:755-759.
26. Menotta M, Biagiotti S, Bartolini G, et al. Nano-mechanical characterization of ataxia telangiectasia cells treated with dexamethasone. *Cell Biochem Biophys*. 2017;75:95-102.
27. Biagiotti S, Menotta M, Orazi S, et al. Dexamethasone improves redox state in ataxia telangiectasia cells by promoting an NRF2-mediated antioxidant response. *FEBS J*. 2016;283:3962-3978.
28. Li J, Chen J, Ricupero CL, et al. Nuclear accumulation of HDAC4 in ATM deficiency promotes neurodegeneration in ataxia telangiectasia. *Nat Med*. 2012;18:783-790.
29. Sando R 3rd, Gounko N, Pieraut S, Liao L, Yates J 3rd, Maximov A. HDAC4 governs a transcriptional program essential for synaptic plasticity and memory. *Cell*. 2012;151:821-834.
30. Darcy MJ, Calvin K, Cavnar K, Ouimet CC. Regional and subcellular distribution of HDAC4 in mouse brain. *J Comp Neurol*. 2010;518:722-740.
31. Broide RS, Redwine JM, Aftahi N, Young W, Bloom FE, Winrow CJ. Distribution of histone deacetylases 1–11 in the rat brain. *J Mol Neurosci*. 2007;31:47-58.
32. Wang AH, Kruhlak MJ, Wu J, et al. Regulation of histone deacetylase 4 by binding of 14-3-3 proteins. *Mol Cell Biol*. 2000;20:6904-6912.
33. Nishino TG, Miyazaki M, Hoshino H, Miwa Y, Horinouchi S, Yoshida M. 14-3-3 regulates the nuclear import of class IIa histone deacetylases. *Biochem Biophys Res Comm*. 2008;377:852-856.
34. Grozinger CM, Schreiber SL. Regulation of histone deacetylase 4 and 5 and transcriptional activity by 14-3-3-dependent cellular localization. *Proc Natl Acad Sci USA*. 2000;97:7835-7840.
35. Paroni G, Cernotta N, Dello Russo C, et al. PP2A regulates HDAC4 nuclear import. *Mol Biol Cell*. 2008;19:655-667.
36. Menotta M, Biagiotti S, Spapperi C, et al. ATM splicing variants as biomarkers for low dose dexamethasone treatment of A-T. *Orphanet J Rare Dis*. 2017;12:126.
37. Laemmli UK. Cleavage of structural proteins during the assembly of the head of bacteriophage T4. *Nature*. 1970;227:680-685.
38. Ladner CL, Yang J, Turner RJ, Edwards RA. Visible fluorescent detection of proteins in polyacrylamide gels without staining. *Anal Biochem*. 2004;326:13-20.
39. Gilda JE, Gomes AV. Stain-Free total protein staining is a superior loading control to beta-actin for Western blots. *Anal Biochem*. 2013;440:186-188.

40. Romero-Calvo I, Ocon B, Martinez-Moya P, et al. Reversible Ponceau staining as a loading control alternative to actin in Western blots. *Anal Biochem*. 2010;401:318-320.
41. Napione L, Pavan S, Veglio A, et al. Unraveling the influence of endothelial cell density on VEGF-A signaling. *Blood*. 2012;119:5599-5607.
42. Matsushima S, Kuroda J, Ago T, et al. Increased oxidative stress in the nucleus caused by Nox4 mediates oxidation of HDAC4 and cardiac hypertrophy. *Circ Res*. 2013;112:651-663.
43. Ago T, Liu T, Zhai P, et al. A redox-dependent pathway for regulating class II HDACs and cardiac hypertrophy. *Cell*. 2008;133:978-993.
44. Rybak JN, Scheurer SB, Neri D, Elia G. Purification of biotinylated proteins on streptavidin resin: a protocol for quantitative elution. *Proteomics*. 2004;4:2296-2299.
45. Menotta M, Crinelli R, Carloni E, et al. Label-free quantification of activated NF-kappaB in biological samples by atomic force microscopy. *Biosens Bioelectron*. 2010;25:2490-2496.
46. Mielcarek M, Zielonka D, Carnemolla A, Marcinkowski JT, Guidez F. HDAC4 as a potential therapeutic target in neurodegenerative diseases: a summary of recent achievements. *Front Cell Neurosci*. 2015;9:42.
47. Di Giorgio E, Brancolini C. Regulation of class IIa HDAC activities: it is not only matter of subcellular localization. *Epigenomics*. 2016;8:251-269.
48. Wang Z, Qin G, Zhao TC. HDAC4: mechanism of regulation and biological functions. *Epigenomics*. 2014;6:139-150.
49. Mani M, Khaghani S, Gol Mohammadi T, et al. Activation of Nrf2-antioxidant response element mediated glutamate cysteine ligase expression in hepatoma cell line by homocysteine. *Hepat Mon*. 2013;13:e8394.
50. Venugopal R, Jaiswal AK. Nrf1 and Nrf2 positively and c-Fos and Fra1 negatively regulate the human antioxidant response element-mediated expression of NAD(P)H:quinone oxidoreductase1 gene. *Proc Natl Acad Sci USA*. 1996;93:14960-14965.
51. Singh A, Happel C, Manna SK, et al. Transcription factor NRF2 regulates miR-1 and miR-206 to drive tumorigenesis. *J Clin Investig*. 2013;123:2921-2934.
52. Mihaylova MM, Vasquez DS, Ravnskjaer K, et al. Class IIa histone deacetylases are hormone-activated regulators of FOXO and mammalian glucose homeostasis. *Cell*. 2011;145:607-621.
53. Guenther MG, Barak O, Lazar MA. The SMRT and N-CoR corepressors are activating cofactors for histone deacetylase 3. *Mol Cell Biol*. 2001;21:6091-6101.
54. Maxwell PH, Pugh CW, Ratcliffe PJ. Activation of the HIF pathway in cancer. *Curr Opin Genet Dev*. 2001;11:293-299.
55. Semenza GL. Hypoxia-inducible factor 1: regulator of mitochondrial metabolism and mediator of ischemic preconditioning. *Biochem Biophys Acta*. 2011;1813:1263-1268.
56. Tang Y, Liu S, Li N, et al. 14-3-3zeta promotes hepatocellular carcinoma venous metastasis by modulating hypoxia-inducible factor-1alpha. *Oncotarget*. 2016;7:15854-15867.
57. Brugarolas J, Lei K, Hurley RL, et al. Regulation of mTOR function in response to hypoxia by REDD1 and the TSC1/TSC2 tumor suppressor complex. *Genes Dev*. 2004;18:2893-2904.
58. D'Assante R, Fusco A, Palamaro L, et al. Abnormal cell-clearance and accumulation of autophagic vesicles in lymphocytes from patients affected with Ataxia-Teleangiectasia. *Clin Immunol*. 2017;175:16-25.
59. Kong D, Park EJ, Stephen AG, et al. Echinomycin, a small-molecule inhibitor of hypoxia-inducible factor-1 DNA-binding activity. *Cancer Res*. 2005;65:9047-9055.
60. Sofer A, Lei K, Johannessen CM, Ellisen LW. Regulation of mTOR and cell growth in response to energy stress by REDD1. *Mol Cell Biol*. 2005;25:5834-5845.
61. Qiao S, Dennis M, Song X, et al. A REDD1/TXNIP pro-oxidant complex regulates ATG4B activity to control stress-induced autophagy and sustain exercise capacity. *Nat Commun*. 2015;6:7014.
62. Molitoris JK, McColl KS, Swerdlow S, et al. Glucocorticoid elevation of dexamethasone-induced gene 2 (Dig2/RTP801/REDD1) protein mediates autophagy in lymphocytes. *J Biol Chem*. 2011;286:30181-30189.
63. Xilouri M, Stefanis L. Autophagy in the central nervous system: implications for neurodegenerative disorders. *CNS Neurol Disord: Drug Targets*. 2010;9:701-719.
64. Kabeya Y, Mizushima N, Ueno T, et al. LC3, a mammalian homologue of yeast Apg8p, is localized in autophagosome membranes after processing. *EMBO J*. 2000;19:5720-5728.
65. Tanida I, Ueno T, Kominami E. LC3 and autophagy. *Methods Mol Biol*. 2008;445:77-88.
66. Tanida I, Minematsu-Ikeguchi N, Ueno T, Kominami E. Lysosomal turnover, but not a cellular level, of endogenous LC3 is a marker for autophagy. *Autophagy*. 2005;1:84-91.
67. Kuma A, Matsui M, Mizushima N. LC3, an autophagosome marker, can be incorporated into protein aggregates independent of autophagy: caution in the interpretation of LC3 localization. *Autophagy*. 2007;3:323-328.
68. Mizushima N, Yoshimori T. How to interpret LC3 immunoblotting. *Autophagy*. 2007;3:542-545.
69. Bjorkoy G, Lamark T, Brech A, et al. p62/SQSTM1 forms protein aggregates degraded by autophagy and has a protective effect on huntingtin-induced cell death. *J Cell Biol*. 2005;171:603-614.
70. Liang C, Lee JS, Inn KS, et al. Beclin1-binding UVRAG targets the class C Vps complex to coordinate autophagosome maturation and endocytic trafficking. *Nat Cell Biol*. 2008;10:776-787.
71. Nickerson DP, Brett CL, Merz AJ. Vps-C complexes: gatekeepers of endolysosomal traffic. *Curr Opin Cell Biol*. 2009;21:543-551.
72. Peng C, Ye J, Yan S, et al. Ablation of vacuole protein sorting 18 (Vps18) gene leads to neurodegeneration and impaired neuronal migration by disrupting multiple vesicle transport pathways to lysosomes. *J Biol Chem*. 2012;287:32861-32873.
73. Dennis PB, Jaeschke A, Saitoh M, Fowler B, Kozma SC, Thomas G. Mammalian TOR: a homeostatic ATP sensor. *Science*. 2001;294:1102-1105.
74. Fingar DC, Blenis J. Target of rapamycin (TOR): an integrator of nutrient and growth factor signals and coordinator of cell growth and cell cycle progression. *Oncogene*. 2004;23:3151-3171.
75. Wolff NC, McKay RM, Brugarolas J. REDD1/DDIT4-independent mTORC1 inhibition and apoptosis by glucocorticoids in thymocytes. *Mol Cancer Res*. 2014;12:867-877.
76. Wang H, Kubica N, Ellisen LW, Jefferson LS, Kimball SR. Dexamethasone represses signaling through the mammalian target of rapamycin in muscle cells by enhancing expression of REDD1. *J Biol Chem*. 2006;281:39128-39134.
77. Polman JA, Hunter RG, Speksnijder N, et al. Glucocorticoids modulate the mTOR pathway in the hippocampus: differential effects depending on stress history. *Endocrinology*. 2012;153:4317-4327.

78. Flynn P, Wongdagger M, Zavar M, Dean NM, Stokoe D. Inhibition of PDK-1 activity causes a reduction in cell proliferation and survival. *Curr Biol*. 2000;10:1439-1442.
79. Scheid MP, Marignani PA, Woodgett JR. Multiple phosphoinositide 3-kinase-dependent steps in activation of protein kinase B. *Mol Cell Biol*. 2002;22:6247-6260.
80. Sarbassov DD, Guertin DA, Ali SM, Sabatini DM. Phosphorylation and regulation of Akt/PKB by the rictor-mTOR complex. *Science*. 2005;307:1098-1101.
81. Matthews L, Berry A, Ohanian V, Ohanian J, Garside H, Ray D. Caveolin mediates rapid glucocorticoid effects and couples glucocorticoid action to the antiproliferative program. *Mol Endocrinol*. 2008;22:1320-1330.
82. Jewell JL, Guan KL. Nutrient signaling to mTOR and cell growth. *Trends Biochem Sci*. 2013;38:233-242.
83. Saxton RA, Sabatini DM. mTOR signaling in growth, metabolism, and disease. *Cell*. 2017;169:361-371.
84. Endo H, Nito C, Kamada H, Yu F, Chan PH. Akt/GSK3beta survival signaling is involved in acute brain injury after subarachnoid hemorrhage in rats. *Stroke*. 2006;37:2140-2146.
85. Dennis MD, McGhee NK, Jefferson LS, Kimball SR. Regulated in DNA damage and development 1 (REDD1) promotes cell survival during serum deprivation by sustaining repression of signaling through the mechanistic target of rapamycin in complex 1 (mTORC1). *Cell Signal*. 2013;25:2709-2716.
86. Kimura S, Noda T, Yoshimori T. Dynein-dependent movement of autophagosomes mediates efficient encounters with lysosomes. *Cell Struct Funct*. 2008;33:109-122.
87. Du F, Sun L, Chu Y, et al. DDIT4 promotes gastric cancer proliferation and tumorigenesis through the p53 and MAPK pathways. *Cancer Commun*. 2018;38:45.

SUPPORTING INFORMATION

Additional supporting information may be found online in the Supporting Information section.

How to cite this article: Ricci A, Galluzzi L, Magnani M, Menotta M. DDIT4 gene expression is switched on by a new HDAC4 function in ataxia telangiectasia. *The FASEB Journal*. 2020;34:1802–1818. https://doi.org/10.1096/fj.201902039R